

Deuteration of Aromatic Rings under Very Mild Conditions through Keto-Enamine Tautomeric Amplification

S. Hessam M. Mehr,[†] Katsuya Fukuyama,[‡] Stephanie Bishop,[†] Francesco Lejl,^{*,§} and Mark J. MacLachlan^{*,†}

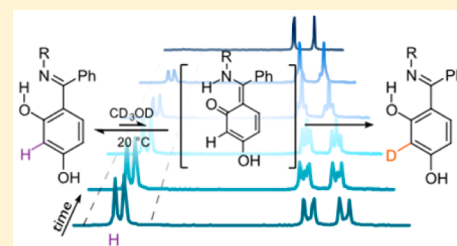
[†]Department of Chemistry, The University of British Columbia, 2036 Main Mall, Vancouver, British Columbia V6T 1Z1, Canada

[‡]Center for Liberal Arts, Meiji Gakuin University, Yokohama 244-8539, Japan

[§]Department of Scienze and LaSCaMM of INSTM, Università della Basilicata, 85100 Potenza, Italy

Supporting Information

ABSTRACT: We have discovered a surprising, mild method for deuteration of select aromatic compounds that is facilitated by a keto-enamine tautomeric intermediate. The mechanism of the reaction has been studied using kinetics experiments and detailed computational analysis. It was found that a chain of water molecules has a substantial role in lowering the activation barrier to the tautomerization-enhanced deuteration reaction. Our results demonstrate that tautomeric forms of aromatic molecules can be exploited to bring about enhanced reactivity.



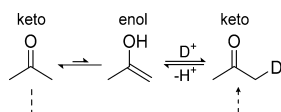
INTRODUCTION

Deuterium-labeled compounds are widely used as NMR solvents and as standards in analytical chemistry.¹ Selective deuteration is also crucial for elucidating reaction mechanisms, characterizing complex products, and identifying new transformations.² Many biological studies use deuterated compounds to monitor metabolic pathways in organisms.³ However, deuterated compounds are generally difficult and expensive to produce directly, owing to the low natural abundance of ²D (ca. 0.02% of H).

Deuteration of aromatic compounds is generally achieved through H/D exchange,⁴ where transition metal catalysis is most commonly employed to lower the activation barrier.^{5–7} In the absence of transition metal catalysts, these reactions often require high temperatures or strong acids or bases.^{8–10} Indeed, aniline and phenol have long been known to undergo H/D exchange at the ortho and para positions on prolonged heating with acid and base, respectively.^{11,12} Due to the harsh conditions required, these catalyst-free methods are usually not very selective and are incompatible with many functional groups.

Tautomerism, the rapid interconversion of different structural forms of a molecule, is ubiquitous in organic chemistry and underlies much of the chemistry of carbonyl compounds, including H/D exchange, Scheme 1.¹³ Tautomerism can be a

Scheme 1. Deuteration of Acetone, Shown Here in Acidic Media, Involves an Enolic Intermediate



powerful synthetic tool, as the different tautomers of the same molecule can have distinct reactivities. Indeed, electrophilic deuteration of aldehydes, ketones, phenols, and anilines all proceed thanks to keto–enol tautomerism.

While investigating new Schiff base macrocycles, we noticed on several occasions that some aromatic resonances were missing in their ¹H NMR spectra. Upon further study, we discovered that our macrocycles based on Schiff bases of 4,6-diformylresorcinol undergo selective D-incorporation on the aromatic ring upon standing in methanol-*d*₄ (CD₃OD), accounting for the loss in intensity of the corresponding ¹H NMR peak.¹⁴ Surprisingly, the reaction proceeds at room temperature even in the absence of catalyst.

Here, we report our findings on the mechanism of this transformation as well as its application to incorporate deuterium into select aromatic systems. In particular, we demonstrate that keto-enamine tautomerization between substituents on the ring is largely responsible for facilitating H/D exchange. We further show that some salicylaldehyde derivatives can be selectively deuterated using catalytic amounts of amine.

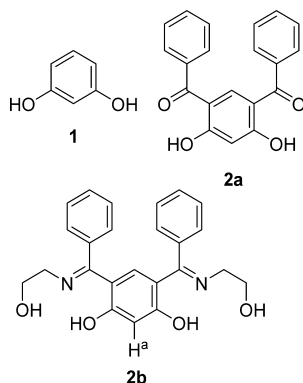
RESULTS AND DISCUSSION

We observed no deuteration of model compounds resorcinol (1) or 4,6-dibenzoylresorcinol (2a) in CD₃OD over a period of 1 week at room temperature. In contrast, in Schiff base 2b the exchange of H^a with deuterium occurs with a half-life of 127 h at room temperature. The deuteration is selective, and only the hydrogen atom labeled H^a is exchanged (in addition to the hydroxyl groups, of course; the rapid and ubiquitous exchange

Received: March 10, 2015

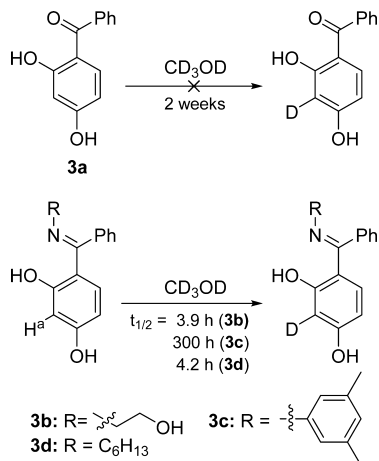
Published: April 23, 2015

of alcohol hydrogens has been neglected in the structures to follow and in the schemes for the sake of clarity).



We next turned our attention to compounds that have a single ketimine functionality in order to determine the minimum structural requirements for this mild deuteration. Thus, in CD_3OD , compound **3a** undergoes no deuteration over 2 weeks, whereas ketimines **3b**, **3c**, and **3d** all show deuteration at room temperature without added acid or base catalyst ($t_{1/2} = 3.9, 300,$ and 4.2 h, respectively). As with compound **2b**, the deuteration is very selective, occurring only between the two hydroxyl substituents on the ring, Scheme 2.

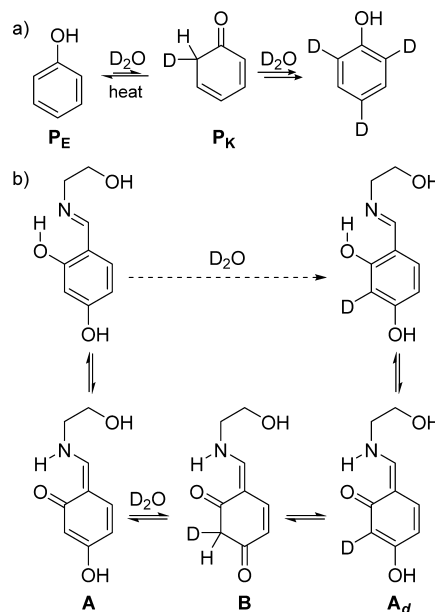
Scheme 2. Rapid and Selective Deuteration of 3b, 3c, and 3d at the H^a Position in CD_3OD at Room Temperature^a



^aCompound **3a** does not undergo H/D exchange under the same conditions ($t_{1/2} \gg 2$ weeks).

The rapid exchange of hydrogen atom H^a in compounds **3b–d** under such mild conditions was surprising to us. For phenols, the incorporation of deuterium into the aromatic ring at high temperature is thought to proceed through the tautomerization to the keto form P_K of the principal enol structure, P_E , shown in Scheme 3a. This transformation disrupts aromaticity in the benzene ring and is strongly disfavored,¹⁵ hence the requirement for elevated temperatures. Schiff bases based on salicylaldehyde, on the other hand, are known to tautomerize to keto-enamine forms with diminished aromaticity.^{16–19} This diminished aromatic character can presumably lower the energetic cost of the keto-mediated H/D exchange pathway described above. In this case, the keto-enamine tautomer **A** facilitates the formation of the all-keto form **B**, thereby enabling H/D exchange under milder conditions, Scheme 3b. This can

Scheme 3. (a) H/D Exchange in Phenol Requires High Temperatures and Proceeds through Keto-Enol Tautomerization and (b) The Same Tautomeric Conversion in Compound 3b Is Amplified by an Initial Transformation to the Keto-Enamine Tautomer



be interpreted as the keto–enol tautomerism of the phenolic moiety at the 4 position, which is normally not observed due to unfavorable energetics, being “amplified” by the preceding intramolecular transformation to keto-enamine **A**.

Study of H/D Exchange by NMR Spectroscopy and Mass Spectrometry. The progress of the exchange reaction can be followed using ^1H NMR spectroscopy. One can monitor the fraction of deuterium-exchanged substrate by integrating the peak for the exchanging proton against a reference proton peak from the same molecule. The choice of reference is immaterial since the integrated areas of all nonexchanging peaks remain constant through the experiment. As Figure 1 demonstrates, the reaction follows first-order kinetics. Similar behavior was observed for all species in this study that underwent H/D exchange.

The incorporation of deuterium into the aromatic ring was also confirmed using high-resolution ESI mass spectrometry. A sample of **3b** was stored in CD_3OD until fully deuterated; CD_3OD was then removed under reduced pressure and replaced with regular methanol shortly before sample analysis. In this manner, we ensure that the hydroxyl groups have been converted back to the protiated OH form while the aromatic deuterium is still present thanks to the smaller rate of exchange at this position. The resulting mass spectrum shows mainly a peak $m/z = 259.1084$, corresponding to $(\text{3b-}d_1 + \text{H})^+$ (calculated 259.1187). This experiment further confirms that a single site that is not rapidly exchanged with MeOH has indeed been exchanged, consistent with the ^1H NMR data.

Mechanistic Investigations. In order to further probe the mechanism, we synthesized compounds **4** and **5** as analogues of **3b** that have one of their phenol groups protected. Compound **4** can undergo enol-imine/keto-enamine tautomerization, but the methyl group should inhibit the keto/enol tautomerization needed for deuteration. On the other hand, compound **5** can, in principle, still undergo the keto/enol tautomerization required

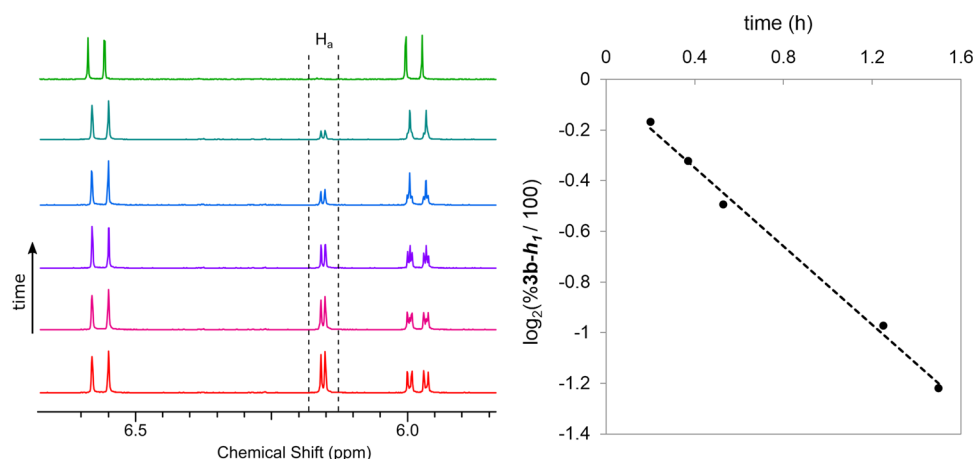
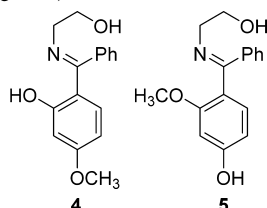


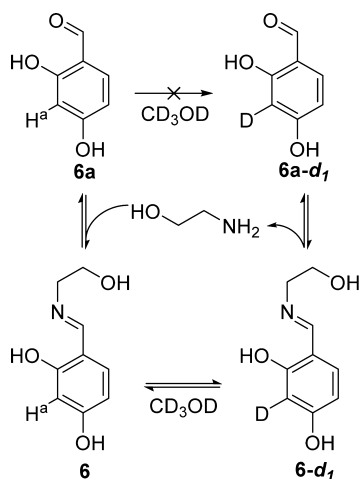
Figure 1. The exchange reaction for **3b** was monitored using ^1H NMR spectroscopy by plotting the area of the H^a peak (Scheme 2) relative to a reference proton in the molecule. This value corresponds to the fraction of the undeuterated form, $3b\text{-}h_1$, and when plotted on a logarithmic scale, gives a straight line, confirming first order kinetics.

for deuteration, but we expected that the rate would be substantially reduced because the added methyl group precludes the formation of the keto-enamine tautomer and the associated tautomeric amplification. Consistent with our proposed mechanism, neither of these compounds underwent deuterium exchange ($t_{1/2} \gg 2$ weeks) in CD_3OD .



The deuteration reaction is not limited to ketimine compounds; it also applies to aldimines. Furthermore, since the formation of aldimines is reversible under the conditions of H/D exchange, it is possible to use catalytic quantities of amine. For instance, adding 0.25 equiv of ethanolamine to a solution of **6a** in CD_3OD brought about the exchange of H^a with a half-life of about 50 h at room temperature (Scheme 4). No exchange was observed before the amine was added. The apparent

Scheme 4. Catalytic Amounts of Ethanolamine Can Affect H/D Exchange in **6a** through Reversible Formation of Schiff Base **6**



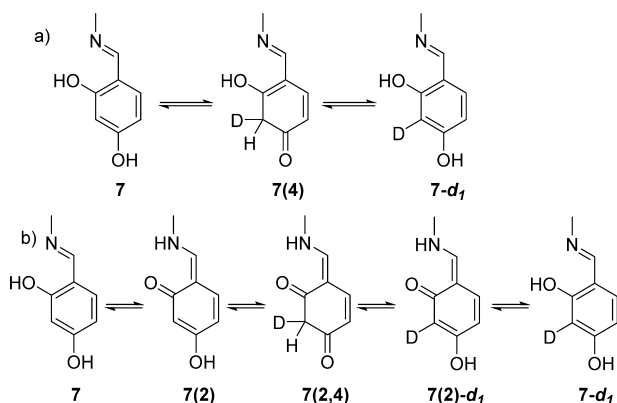
catalytic behavior of the amine in this case can be attributed to the reversible formation of Schiff base **6**, which can undergo H/D exchange in the same fashion as the ketimines.

Through the course of our experiments, we observed that the rate of deuterium incorporation is highly solvent-dependent. Specifically, using D_2O instead of CD_3OD caused a large increase in the rate of deuteration. In fact, in many cases the reaction is too fast in D_2O to follow using NMR spectroscopy at room temperature. This rate enhancement is possible even in cases where the compound is not soluble in water simply by shaking a chloroform solution of the compound with D_2O . Furthermore, considering the fact that NMR-grade $\text{MeOH-}d_4$ contains trace amounts of water, it is possible that the mechanism directly involves water molecules in both solvents. We expect D_2O to be the solvent of choice where rapid exchange is desired.

Ab Initio Studies of Reaction Mechanism. In order to verify the proposed mechanism and elucidate the role of solvent, we undertook an extensive ab initio computational study of H/D exchange in model compound **7** at various levels of theory. In principle, compound **7** can directly undergo keto-enol tautomerization in its native form to yield **7(4)**, as in Scheme 5a. The alternative, shown in Scheme 5b, is to go through the keto-enamine form **7(2)**. If tautomeric amplification is responsible for the observed reactivity, then it is expected that this indirect mechanism will possess favorable energetics.

The calculated energies of the intermediates relative to **7** unequivocally show that **7(4)** ($E = 51.3$ kJ/mol) is too unstable to be involved. In contrast, both **7(2)** ($E = 2.9$ kJ/mol) and **7(2,4)** ($E = 8.9$ kJ/mol) are reasonable intermediates for a room-temperature reaction. Furthermore, **7(2)** can be reached through a simple intramolecular rearrangement from **7** with activation energy $E^\ddagger = 39.5$ kJ/mol.

We looked for a similar intramolecular transition state for the transformation of **7(2)** to **7(2,4)** using a continuum model of the solvent, but we found a high activation barrier of more than 239 kJ/mol. On the other hand, water molecules have been used to mediate proton transfer in earlier ab initio studies of tautomerism, yielding much lower activation energies.^{20,21} Guided by this and the experimental observation that H/D exchange is faster in the presence of water, we hypothesized

Scheme 5. Two Proposed Mechanisms for H/D Exchange in Model Compound 7^a

^aKeto-enol tautomerism can proceed at the enol-imine (a) or keto-enamine (b) stage. (Hydrogen atoms rather than deuteriums were used for all calculated structures.)

that proton transfer is mediated by a hydrogen-bonded network of water molecules.

As expected, a larger number of water molecules can lead to a more stable transition state, at the cost of longer calculation times. A hydrogen-bonded framework of five water molecules is computationally tractable even when electronic correlation is included and can afford activation barriers as low as 114 kJ/mol. In the first step of this calculated mechanism, the phenol proton moves to nearby water molecule w_a in a barrierless process, Figure 2a. This water molecule then protonates water

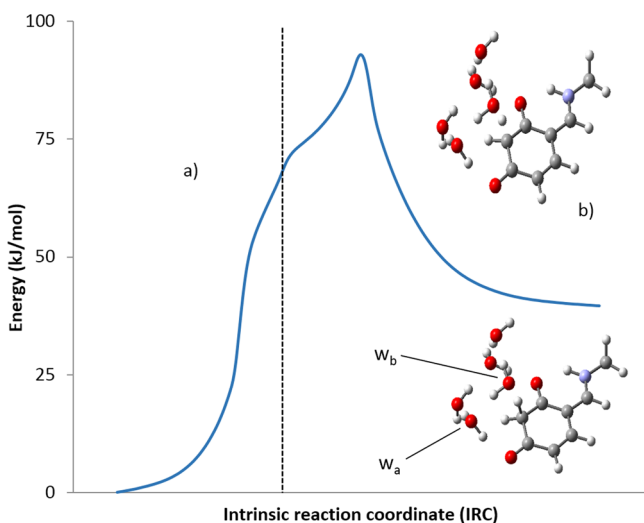


Figure 2. Energy versus intrinsic reaction coordinate (IRC) for the transformation of 7(2) to 7(2,4) mediated by water molecules. The dotted line indicates the region where the phenolic hydrogen atom moves to w_a without engendering any high-energy intermediate.

molecule w_b , which is situated closer to the CH at the 3 position. Concurrently with this latter step, a proton moves from w_b to the CH, Figure 2b. This particular hydrogen-bonded framework seems to be indispensable, as repeating the calculation using fewer than five water molecules raises the activation energy significantly.

Our calculations also suggest that the rate of deuteration is strongly dependent on the arrangement of the OH substituents

around the aromatic ring. To test this experimentally, we investigated the deuteration of compounds 8–10 shown in Figure 3, which were prepared in situ by combining the

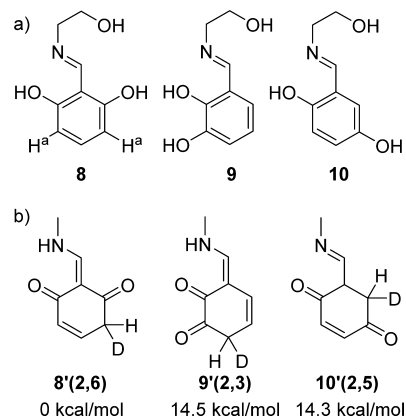


Figure 3. (a) Compound 8 shows deuteration of the H^a positions under mild conditions, whereas compounds 9 and 10 do not undergo facile deuteration. (b) Energy values of the all-keto intermediates relative to the all-enol form for the computational analogues of compounds 8–10. (Note that the calculations were performed with H atoms in the place of D.)

corresponding aldehydes with ethanolamine. Of these Schiff bases, only compound 8 shows the same mild deuteration behavior as that of 3b at the positions labeled H^a . Our ab initio calculations on simplified analogues of these compounds, 8'–10', are consistent with this observation. Intermediate species 9'(2,3) and 10'(2,5) are less stable than the corresponding starting materials by more than 58 kJ/mol, whereas 8'(2,6) is just as stable as the starting material.

In accordance with our experimental results, it appears that a 1,3-arrangement of hydroxyl groups on the benzene ring is critical to facile deuteration. Furthermore, in the case of 8'(2), a very similar system of water molecules as the one described above can mediate proton transfer and provide a low-energy pathway to 8'(2,6).

Computational results confirm the proposed reaction mechanism and help to explain the observed regio- and chemoselectivity. On the basis of the results, the striking reactivity difference between imine and carbonyl is linked to the facile formation of the intermediate keto-enamine tautomers, e.g., 7(2), and their stabilization of the nonaromatic all-keto intermediates, e.g., 7(2,4).

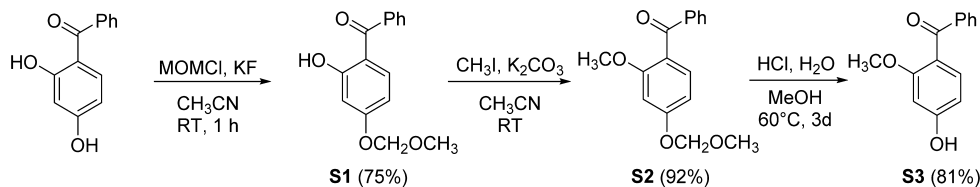
CONCLUSIONS

In conclusion, we have leveraged an intramolecular interaction to amplify the tautomerism of phenols to their keto form. This amplification served to alter the reactivity of the phenol, in this case providing a mild, rapid, and selective method for deuterium incorporation in aromatic rings. We expect that our understanding of the mechanism will pave the way to the design of other tautomeric species with novel and exceptional reactivity.

EXPERIMENTAL SECTION

Computational Study. All ab initio calculations were performed using Gaussian09²² using the 6-311G(d,p)²³ basis set. All calculations were performed in bulk solvent as described by the polarizable continuum model (PCM).²⁴ In some cases, we found it necessary to

Scheme 6. New Route to 4-Hydroxy-2-methoxybenzophenone



explicitly include solvent molecules in addition to bulk PCM solvent to mediate proton transfer.

Fourth-order Møller–Plesset theory (MP4)^{25,26} was used throughout for the calculation of the single-point energies of previously energy-optimized geometries. When no more than one explicit solvent (water) molecule was included in the calculation, it was feasible to use MP4 for geometry optimizations as well. In these cases, optimizations were performed using MP4 including double and quadruple substitution, MP4(DQ), with single, double, triple, and quadruple substitutions (SDTQ) reserved for the calculation of single-point energies. The Minnesota 06 (M06) functional²⁷ was used in preliminary explorations, although calculated reaction energetics vary widely between M06 and MP4.

With the inclusion of more than one explicit water molecule, density function theory (DFT) using the double-hybrid MPW2PLYP functional²⁸ was used as a less expensive alternative to MP4 for geometry optimization. Single-point energies were still calculated using MP4 but at the MP4(DQ) level.

Kinetics Study. Longitudinal relaxation times (T_1) for the compounds under study were first measured in an inversion recovery experiment, and the recycle delay was set to $5 \times T_1$ to ensure complete relaxation of the nuclei and accurate peak areas.

For all but the exchanging protons, peak areas consistently correspond to their expected values (within 5% error). Therefore, any number of peaks can be used as integration reference, i.e., identical kinetics data is obtained regardless of the choice of reference.

For kinetics experiments on reversibly formed aldimines, the aldehyde starting material was added to an NMR tube containing a small amount, typically 0.2 equiv, of ethanolamine in CD_3OD . The exact ratio of aldehyde to ethanolamine was determined by comparing the relative integration of the carbonyl proton to the ethanolamine CH_2 peaks. Schiff base formation is essentially complete in under an hour, but this induction period was not taken into account in half-life calculations.

Materials. 2,6-Dihydroxybenzaldehyde was prepared using literature methods.^{29,30} 4-Hydroxy-2-methoxybenzophenone, while known, was synthesized by the new route shown in Scheme 6 and described below. 3,5-Dimethylaniline was distilled over KOH under reduced pressure to give a pale yellow liquid. 2,5-Dihydroxybenzaldehyde was purified by filtering a dichloromethane solution of the compound followed by evaporating the filtrate to give a bright yellow solid.

Preparation of 4-Hydroxy-2-methoxybenzophenone. Step 1: 2-Hydroxy-4-(methoxymethoxy)benzophenone (S1). **Caution:** Chloromethyl methyl ether is highly toxic, flammable, and a known human carcinogen. Consult the material safety data sheet (MSDS) before use.

2,4-Dihydroxybenzophenone (2.00 g, 9.3 mmol) and KF (1.10 g, 19 mmol, 2 equiv) were heated under vacuum at 80 °C for 30 min to remove any moisture. Acetonitrile (20 mL, dried over Linde 4 Å molecular sieves) was added next, giving a bright yellow solution. Injecting chloromethyl methyl ether (1.56 mL, 20.5 mmol, 2.2 equiv) causes the yellow color to disappear immediately. Thin-layer chromatography (TLC) showed that most of the starting material, R_f 0.2 (dichloromethane), was converted to product, R_f 0.8 (dichloromethane), within an hour. Solvent was removed under reduced pressure at room temperature before adding 100 mL of saturated sodium bicarbonate solution and extracting the product twice with 25 mL of dichloromethane. The organic layer was washed twice with deionized water and dried over sodium sulfate, leaving an

amber oil after removal of solvent. The remaining starting material was removed by passing the product through a pad of silica gel using dichloromethane as eluent. The title compound is thus obtained as 1.75 g (6.7 mmol, 75%) of a light yellow oil that turns into a waxy solid upon standing. mp 55–57 °C. 1H NMR (300 MHz, $CDCl_3$) δ 12.53 (s, 1H; OH), 7.65 (m, 2H; Ar), 7.53 (m, 4H; Ar), 6.70 (d, $^3J_{HH} = 2.4$ Hz, 1H; Ar), 6.53 (dd, $^3J_{HH} = 9.0, 2.4$ Hz, 1H; Ar), 5.24 (s, 2H; CH_2), 3.50 (s, 3H; CH_3). ^{13}C NMR (100 MHz, $CDCl_3$) δ 200.1, 165.8, 163.6, 138.2, 135.3, 131.5, 128.9, 128.3, 113.9, 107.9, 103.9, 94.0, 56.4. UV–vis (MeOH) $\lambda_{max}(\epsilon) = 328 (7.1 \times 10^3), 286 (9.1 \times 10^3), 244 (7.6 \times 10^3), 223 (7.9 \times 10^3)$ nm ($cm^{-1} mol^{-1} L$). IR (neat) $\nu = 2930, 2830, 1621, 1592, 1574, 1504, 1445, 1421, 1346, 1250, 1230, 1217, 1152, 1119, 1074, 983, 951, 928, 909, 840, 802, 784, 697, 639$ cm^{-1} . HRMS (ESI/TOF) m/z : $[S1 + Na]^+$ calcd for $C_{15}H_{14}O_4Na$, 281.0790; found, 281.0792.

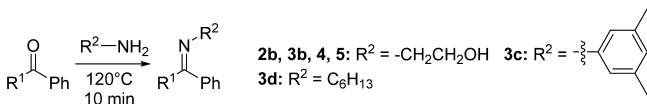
Step 2: 2-Methoxy-4-(methoxymethoxy)benzophenone (S2). Potassium carbonate (3.30 g, 23.9 mmol, 3.5 equiv) was added to a solution of 2-hydroxy-4-(methoxymethoxy)benzophenone (1.75 g, 6.78 mmol) in 20 mL of dry acetonitrile, causing the pale yellow color of the starting material to intensify. After 1 h of stirring, 1.5 mL of iodomethane (24 mmol, 3.5 equiv) was added, the flask was sealed, and the reaction was allowed to progress at room temperature overnight. TLC showed that most of the starting material, $R_f = 0.8$ (dichloromethane), had been converted to product, $R_f = 0.3$ (dichloromethane), after 12 h. To affect complete conversion, an extra 0.70 mL (11 mmol, 1.7 equiv) of CH_3I and 1.5 g (11 mmol, 1.7 equiv) of potassium carbonate were added at that point. The progress of the reaction was followed by monitoring the yellow color of the starting material anion, which completely disappeared in about 12 h. Next, solvent was removed under reduced pressure, and the product was dissolved in dichloromethane. This dichloromethane solution was washed with distilled water, dried over $MgSO_4$, and evaporated, yielding 1.69 g (92%, 6.21 mmol) of the pure product as a colorless oil. 1H NMR (400 MHz, $CDCl_3$) δ 7.79 (m, 2H; Ar), 7.53 (tt, $^3J_{HH} = 7.4, 1.9$ Hz, 1H; Ar), 7.42 (m, 2H; Ar), 7.38 (d, $^3J_{HH} = 8.4, 1H$; Ar), 6.71 (dd, $^3J_{HH} = 8.4, 2.1$ Hz, 1H; Ar), 6.66 (d, $^3J_{HH} = 2.1$ Hz, 1H; Ar), 5.24 (s, 2H; CH_2), 3.70 (s, 3H; CH_3), 3.52 (s, 3H; CH_3). ^{13}C NMR (100 MHz, $CDCl_3$) δ 195.5, 160.8, 159.4, 138.2, 132.4, 131.8, 129.7, 128.0, 122.4, 107.2, 100.3, 94.3, 56.2, 55.5. UV–vis (MeOH) $\lambda_{max}(\epsilon) = 304 (4.4 \times 10^3), 276 (6.1 \times 10^3), 247 (1.2 \times 10^4), 209 (1.4 \times 10^4)$ nm ($cm^{-1} mol^{-1} L$). IR (neat) $\nu = 2938, 2827, 1654, 1600, 1578, 1500, 1463, 1447, 1416, 1315, 1269, 1215, 1192, 1149, 1120, 1076, 1030, 998, 944, 838, 796, 743, 704$ cm^{-1} . HRMS (ESI/TOF) m/z : $[S2 + Na]^+$ calcd for $C_{16}H_{16}O_4Na$, 295.0946; found, 295.0940.

Step 3: 4-Hydroxy-2-methoxybenzophenone (S3). Hydrochloric acid (0.5 mL, 6 mmol, 4 equiv) and water (2 mL) were added to a solution of 2-methoxy-4-(methoxymethoxy)benzophenone (391 mg, 1.43 mmol) in 20 mL of methanol. The solution was heated at 60 °C overnight, during which it developed a pale yellow color. Approximately half of the solvent was removed at room temperature under reduced pressure before adding an extra 5 mL of water and small additions of sodium bicarbonate until the solution pH tested neutral. The remaining methanol was then removed under reduced pressure, and the product was extracted into dichloromethane. The yellow organic layer thus obtained was washed with water, dried over $MgSO_4$, and evaporated to give the pure product as 267 mg (1.17 mmol, 81%) of a thick yellow oil that solidifies upon standing at room temperature. mp 121–123 °C. 1H NMR (400 MHz, $CDCl_3$) δ 7.79 (m, 2H; Ar), 7.55 (tt, $^3J_{HH} = 7.3, 1.2$ Hz, 1H; Ar), 7.43 (m, 2H; Ar), 7.33 (d, $^3J_{HH} = 8.6$ Hz, 1H; Ar), 7.06 (s, 1H; OH), 6.49 (m, 2H; Ar),

3.60 (s, 3H; CH₃). ¹³C NMR (100 MHz, CDCl₃) δ 197.1, 161.4, 160.4, 138.7, 133.1, 132.7, 130.0, 128.1, 119.7, 107.5, 99.5, 55.3. UV-vis (MeOH) λ_{max} (ε) = 311 (6.2 × 10³), 282 (6.5 × 10³), 246 (1.4 × 10⁴), 211 (1.3 × 10⁴) nm (cm⁻¹ mol⁻¹ L). IR (neat) ν = 3335, 1629, 1596, 1573, 1503, 1461, 1350, 1284, 1203, 1110, 1029, 962, 920, 828, 795, 746, 711, 628, 563, 497 cm⁻¹. HRMS (ESI/TOF) *m/z*: [S3 + Na]⁺ calcd for C₁₄H₁₂O₃Na, 251.0684; found, 251.0684.

General Method for the Preparation of Ketimines. All ketimines were prepared by the high-temperature, solvent-free reaction of amine (ethanolamine or 3,5-dimethylaniline) with the appropriate ketone, Scheme 7. In a typical procedure, the ketone and a 10-fold

Scheme 7. Solvent-Free Reaction of Ketone and Imine at High Temperature Generally Yields the Ketimine in Good Yield



excess of amine were combined in a small Schlenk tube, which was purged three times with nitrogen before heating at 120 °C for 10 min to complete the conversion. Depending on the substrate used, most or all of the excess amine could be removed by heating the flask for 12 h at 80 °C under high vacuum. When the product is a glaze, amine removal is much quicker if the glaze is periodically thinned by stirring with methanol or toluene.

Further purification details and characterization data are provided below.

4,6-Dibenzoylresorcinol Ethanolamine Schiff Base (2b). The product was further purified by recrystallization from a mixture of water and methanol, yielding **2b** as a yellow solid in 89% (114 mg from 101 mg of 4,6-dibenzoylresorcinol) yield. Melts with decomposition. ¹H NMR (400 MHz, CD₃OD) δ 7.36 (m, 6H; Ar), 7.13 (d, ³J_{HH} = 7.4 Hz, 4H; Ar), 6.38 (s, 1H; Ar), 5.97 (s, 1H; Ar), 3.70 (t, ³J_{HH} = 5.2 Hz, 4H; CH₂), 3.41 (t, ³J_{HH} = 5.2 Hz, 4H; CH₂). ¹³C NMR (100 MHz, DMSO-*d*₆) δ 173.7, 171.5, 139.0, 131.5, 128.9, 128.2, 127.4, 110.9, 104.9, 60.3, 51.6. UV-vis (MeOH) λ_{max} (ε) = 393 (1.6 × 10⁴), 317 (2.5 × 10⁴) nm (cm⁻¹ mol⁻¹ L). IR (neat) ν = 2900 (br), 1556, 1435, 1301, 1250, 1143, 1080, 938, 919, 840, 782, 756, 705, 669, 591, 566, 467 cm⁻¹. HRMS (ESI/TOF) *m/z*: [2b + H]⁺ calcd for C₂₄H₂₅N₂O₄, 405.1814; found, 405.1812.

2,4-Dihydroxybenzophenone Ethanolamine Schiff Base (3b). All traces of leftover amine were removed by flash column chromatography of the product using 1:9 methanol/dichloromethane. The yellow first fraction was evaporated to give **3b** in 85% (102 mg from 100 mg of 2,4-dihydroxybenzophenone) yield. mp 186–191 °C. ¹H NMR (300 MHz, CD₃OD) δ 7.58 (m, 3H; Ar), 7.36 (m, 2H; Ar), 6.55 (d, ³J_{HH} = 9.0 Hz, 1H; Ar), 6.14 (d, ³J_{HH} = 2.4 Hz, 1H; Ar), 5.96 (dd, ³J_{HH} = 9.0, 2.4 Hz, 1H; Ar), 3.71 (t, ³J_{HH} = 5.4 Hz, 2H; CH₂), 3.40 (t, ³J_{HH} = 5.4 Hz, 2H; CH₂). ¹³C NMR (100 MHz, CD₃OD) δ 177.3, 175.9, 166.3, 135.7, 133.0, 131.0, 129.9, 129.1, 112.0, 107.6, 105.8, 61.6, 50.4. UV-vis (MeOH) λ_{max} (ε) = 384 (8.2 × 10³), 309 (1.5 × 10⁴) nm (cm⁻¹ mol⁻¹ L). IR (neat) ν = 1591, 1573, 1556, 1496, 1471, 1384, 1335, 1260, 1235, 1175, 1118, 1059, 980, 851, 806, 778, 717, 631, 563, 439 cm⁻¹. HRMS (ESI/TOF) *m/z*: [3b + H]⁺ calcd for C₁₅H₁₆NO₃, 258.1130; found, 258.1122.

2,4-Dihydroxybenzophenone 3,5-Dimethylaniline Schiff Base (3c). A yellow-orange solid was obtained in 87% (387 mg from 300 mg of 2,4-dihydroxybenzophenone) yield from the methanol solution by the addition of water. mp 203–205 °C. ¹H NMR (600 MHz, CDCl₃) δ 7.36 (m, 3H; Ar), 7.19 (m, 2H; Ar), 6.93 (d, ³J_{HH} = 8.9 Hz, 1H; Ar), 6.64 (bs, 1H; Ar), 6.55 (d, ³J_{HH} = 2.5 Hz, 1H; Ar), 6.39 (bs, 2H; Ar), 6.25 (dd, ³J_{HH} = 8.9, 2.5 Hz, Ar), 2.14 (s, 6H; CH₃). ¹³C NMR (150 MHz, CDCl₃) δ 171.9, 167.9, 161.5, 144.7, 138.2, 134.3, 133.9, 129.1, 128.9, 128.3, 126.6, 121.0, 113.4, 106.9, 104.4, 21.3. UV-vis (MeOH) λ_{max} (ε) = 403 (shoulder, 3.6 × 10³), 332 (1.3 × 10⁴), 287 (1.2 × 10⁴), 240 (shoulder, 1.5 × 10³) nm (cm⁻¹ mol⁻¹ L). IR (neat) ν = 3351, 2922, 1582, 1442, 1339, 1192, 1112, 1020, 962, 908,

852, 816, 774, 701, 670, 561, 542, 525, 459 cm⁻¹. HRMS (ESI/TOF) *m/z*: [3c + H]⁺ calcd for C₂₁H₂₀NO₂, 318.1490; found, 318.1494.

2,4-Dihydroxybenzophenone Hexylamine Schiff Base (3d). Yellow-orange crystals (270 mg, 84% from 250 mg of 2,4-dihydroxybenzophenone) yield from the cold methanol–water solution. mp 141–147 °C. ¹H NMR (400 MHz, CDCl₃) δ 7.51 (m, 3H; Ar), 7.26 (m, 2H; Ar), 6.55 (d, ³J_{HH} = 9.2 Hz, 1H; Ar), 6.50 (d, ³J_{HH} = 2.6 Hz, 1H; Ar), 6.07 (dd, ³J_{HH} = 9.2, 2.6 Hz, 1H; Ar), 3.21 (t, ³J_{HH} = 7.0 Hz, 2H; CH₂), 1.60 (q, ³J_{HH} = 7.4 Hz, 2H; CH₂), 1.34–1.16 (m, 6H; CH₂), 0.83 (t, ³J_{HH} = 7.0 Hz, 3H; CH₃). ¹³C NMR (75 MHz, CDCl₃) δ 174.8, 173.3, 164.5, 134.0, 132.1, 129.5, 128.6, 127.7, 110.8, 106.9, 105.7, 47.2, 31.3, 30.1, 26.5, 22.4, 14.0. UV-vis (MeOH) λ_{max} (ε) = 337 (7.3 × 10³), 305 (1.2 × 10⁴), 211 (1.3 × 10³) nm (cm⁻¹ mol⁻¹ L). IR (neat) ν = 2954, 2927, 2856, 2550 (br), 1574, 1531, 1488, 1453, 1393, 1340, 1238, 1175, 1113, 1074, 1026, 979, 924, 851, 800, 771, 698, 634, 553 cm⁻¹. HRMS (ESI/TOF) *m/z*: [3d + H]⁺ calcd for C₁₉H₂₄NO₂, 298.1807; found, 298.1807.

2-Hydroxy-4-methoxybenzophenone Ethanolamine Schiff Base (4). A sticky orange-brown solid was obtained in 94% (254 mg from 204 mg of 2-hydroxy-4-methoxybenzophenone) yield that is pure by ¹H NMR spectroscopy. Samples suitable for optical characterization were obtained by passing the product through a short column of silica gel using ethyl acetate as eluent (*R_f* = 0.3) followed by the evaporation of solvent under vacuum. A fluorescent waxy yellow solid was thus obtained in 79% overall yield. ¹H NMR (400 MHz, CD₃OD) δ 7.58 (m, 3H; Ar), 7.35 (m, 2H; Ar), 6.58 (d, ³J_{HH} = 9.2 Hz, 1H; Ar), 6.23 (d, ³J_{HH} = 2.6 Hz, 1H; Ar), 6.04 (dd, ³J_{HH} = 9.2, 2.6 Hz, Ar), 3.77 (s, 3H; CH₃), 3.71 (t, ³J_{HH} = 5.5 Hz, 2H; CH₂), 3.40 (t, ³J_{HH} = 5.5 Hz, 2H; CH₂). ¹³C NMR (100 MHz, acetone-*d*₆) δ 175.1, 168.3, 164.5, 134.9, 133.5, 129.9, 129.6, 128.6, 114.3, 105.8, 102.4, 62.6, 55.7, 54.0. UV-vis (MeOH) λ_{max} (ε) = 387 (2.2 × 10⁴), 305 (3.2 × 10³) nm (cm⁻¹ mol⁻¹ L). IR (neat) ν = 3152, 2951, 2834, 1582, 1538, 1440, 1340, 1221, 1075, 1022, 833, 799, 769, 702, 545, 493 cm⁻¹. HRMS (ESI/TOF) *m/z*: [4 + H]⁺ calcd for C₁₆H₁₈NO₃, 272.1287; found, 272.1282.

4-Hydroxy-2-methoxybenzophenone Ethanolamine Schiff Base (5). The product was obtained in 93% (136 mg from 122 mg of 4-hydroxy-2-methoxybenzophenone) yield as a red glaze. Passing the product through a pad of silica gel using 1:9 methanol/dichloromethane as eluent can yield a bright yellow product, *R_f* = 0.1, suitable for optical characterization, albeit at a lower yield of 45%. ¹H NMR (300 MHz, acetone-*d*₆) δ 7.64 (m, 2H; Ar), 7.32 (m, 3H; Ar), 6.82 (d, ³J_{HH} = 8.1 Hz, 1H; Ar), 6.62 (d, ³J_{HH} = 2.2 Hz, Ar), 6.56 (dd, ³J_{HH} = 8.1 Hz, 2.2 Hz, Ar), 3.77 (t, ³J_{HH} = 6.1 Hz, 2H; CH₂), 3.40 (t, ³J_{HH} = 6.1 Hz, 2H; CH₂). ¹³C NMR (100 MHz, acetone-*d*₆) δ 166.9, 160.2, 158.5, 141.2, 130.01, 129.98, 128.4, 128.3, 117.5, 108.1, 99.7, 63.1, 57.1, 55.7. UV-vis (MeOH) λ_{max} (ε) = 374 (1.6 × 10⁴), 238 (9.3 × 10³) nm (cm⁻¹ mol⁻¹ L). IR (neat) ν = 2930 (br), 1563, 1504, 1366, 1294, 1253, 1200, 1123, 1060, 1027, 958, 836, 774, 697, 590, 548, 511, 456 cm⁻¹. HRMS (ESI/TOF) *m/z*: [5 + H]⁺ calcd for C₁₆H₁₈NO₃, 272.1287; found, 272.1292. Note: Regardless of the purification method used, solutions in acetone-*d*₆ yield clean ¹H NMR spectra, whereas in CDCl₃ and methanol-*d*₄, there appears to be a pair of similar compounds. We suspect this to be due to geometrical isomerism about the C=N double bond.

■ ASSOCIATED CONTENT

Supporting Information

Kinetics data, NMR spectra, expanded ab initio section, and energy-optimized atomic coordinates for all species used in calculations. This material is available free of charge via the Internet at <http://pubs.acs.org>.

■ AUTHOR INFORMATION

Corresponding Authors

*(F.L.) E-mail: francesco.lelj@unibas.it.

*(M.J.M.) E-mail: mmaclach@chem.ubc.ca.

Notes

The authors declare no competing financial interest.

ACKNOWLEDGMENTS

We thank NSERC for supporting this research. F.L. thanks INSTM for financial support for his leave from Italy and the UBC Department of Chemistry for hospitality.

REFERENCES

- (1) Leis, H. J.; Fauler, G.; Windischhofer, W. *Curr. Org. Chem.* **1998**, *2*, 131–144.
- (2) Zimmerman, H. E.; Binkley, R. W.; Givens, R. S.; Sherwin, M. A. *J. Am. Chem. Soc.* **1967**, *89*, 3932–3933.
- (3) Hoshino, M.; Katou, H.; Hagihara, Y.; Hasegawa, K.; Naiki, H.; Goto, Y. *Nat. Struct. Mol. Biol.* **2002**, *9*, 332–336.
- (4) Atzordt, J.; Derdau, V.; Fey, T.; Zimmermann, J. *Angew. Chem., Int. Ed.* **2007**, *46*, 7744–7765.
- (5) Ito, N.; Esaki, H.; Maesawa, T.; Imamiya, E.; Maegawa, T.; Sajiki, H. *Bull. Chem. Soc. Jpn.* **2008**, *81*, 278–286.
- (6) Iluc, V. M.; Fedorov, A.; Grubbs, R. H. *Organometallics* **2012**, *31*, 39–41.
- (7) Parmentier, M.; Hartung, T.; Pfaltz, A.; Muri, D. *Chem.—Eur. J.* **2014**, *20*, 11496–11504.
- (8) Werstiuk, N. H.; Timmins, G. *Can. J. Chem.* **1989**, *67*, 1744–1747.
- (9) Boix, C.; Poliakoff, M. *Tetrahedron Lett.* **1999**, *40*, 4433–4436.
- (10) Junk, T.; Catallo, W. J. *Tetrahedron Lett.* **1996**, *37*, 3445–3448.
- (11) Okazaki, N.; Okumura, A. *Bull. Chem. Soc. Jpn.* **1961**, *34*, 989–995.
- (12) Small, P. A.; Wolfenden, J. H. *J. Chem. Soc.* **1936**, 1811–1817.
- (13) Xu, M.; Wang, W.; Hunger, M. *Chem. Commun.* **2003**, 722–723.
- (14) Jiang, J.; MacLachlan, M. J. *Chem. Commun.* **2009**, 5695–5697.
- (15) Capponi, M.; Gut, I. G.; Hellrung, B.; Persy, G.; Wirz, J. *Can. J. Chem.* **1999**, *77*, 605–613.
- (16) Chong, J. H.; Sauer, M.; Patrick, B. O.; MacLachlan, M. J. *Org. Lett.* **2003**, *5*, 3823–3826.
- (17) Gallant, A. J.; Yun, M.; Sauer, M.; Yeung, C. S.; MacLachlan, M. J. *Org. Lett.* **2005**, *7*, 4827–4830.
- (18) Filarowski, A.; Koll, A.; Sobczyk, L. *Curr. Org. Chem.* **2009**, *13*, 172–193.
- (19) Abood Hameed, S.; Alrouby, S. K.; Hilal, R. *J. Mol. Model.* **2013**, *19*, 559–569.
- (20) Kryachko, E. S.; Nguyen, M. T.; Zeegers-Huyskens, T. *J. Phys. Chem. A* **2001**, *105*, 1934–1943.
- (21) Fogarasi, G. *Chem. Phys.* **2008**, *349*, 204–209.
- (22) Frisch, M. J.; Trucks, G. W.; Schlegel, H. B.; Scuseria, G. E.; Robb, M. A.; Cheeseman, J. R.; Scalmani, G.; Barone, V.; Mennucci, B.; Petersson, G. A.; Nakatsuji, H.; Caricato, M.; Li, X.; Hratchian, H. P.; Izmaylov, A. F.; Bloino, J.; Zheng, G.; Sonnenberg, J. L.; Hada, M.; Ehara, M.; Toyota, K.; Fukuda, R.; Hasegawa, J.; Ishida, M.; Nakajima, T.; Honda, Y.; Kitao, O.; Nakai, H.; Vreven, T.; Montgomery, J. A., Jr.; Peralta, J. E.; Ogliaro, F.; Bearpark, M.; Heyd, J. J.; Brothers, E.; Kudin, K. N.; Staroverov, V. N.; Kobayashi, R.; Normand, J.; Raghavachari, K.; Rendell, A.; Burant, J. C.; Iyengar, S. S.; Tomasi, J.; Cossi, M.; Rega, N.; Millam, J. M.; Klene, M.; Knox, J. E.; Cross, J. B.; Bakken, V.; Adamo, C.; Jaramillo, J.; Gomperts, R.; Stratmann, R. E.; Yazyev, O.; Austin, A. J.; Cammi, R.; Pomelli, C.; Ochterski, J. W.; Martin, R. L.; Morokuma, K.; Zakrzewski, V. G.; Voth, G. A.; Salvador, P.; Dannenberg, J. J.; Dapprich, S.; Daniels, A. D.; Farkas, O.; Foresman, J. B.; Ortiz, J. V.; Cioslowski, J.; Fox, D. J. *Gaussian 09*, revision D.01; Gaussian, Inc.: Wallingford, CT, 2009.
- (23) Krishnan, R.; Binkley, J. S.; Seeger, R.; Pople, J. A. *J. Chem. Phys.* **1980**, *72*, 650–654.
- (24) Tomasi, J.; Mennucci, B.; Cammi, R. *Chem. Rev.* **2005**, *105*, 2999–3093.
- (25) Krishnan, R.; Pople, J. A. *Int. J. Quantum Chem.* **1978**, *14*, 91–100.

(26) Krishnan, R.; Frisch, M. J.; Pople, J. A. *J. Chem. Phys.* **1980**, *72*, 4244–4245.

(27) Zhao, Y.; Truhlar, D. G. *Theor. Chem. Acc.* **2007**, *120*, 215–241.

(28) Schwabe, T.; Grimme, S. *Phys. Chem. Chem. Phys.* **2006**, *8*, 4398–4401.

(29) Dube, H.; Kasumaj, B.; Calle, C.; Felber, B.; Saito, M.; Jeschke, G.; Diederich, F. *Chem.—Eur. J.* **2009**, *15*, 125–135.

(30) Corey, E. J. Ryanodine channel binders and uses thereof. Patent WO2009026444 A1, 2009.